



Supported by



## Accepted Article

**Title:** Bidentate N-based Ligands for Highly Reusable, Ligand-coordinated, Supported Pt Hydrosilylation Catalysts

**Authors:** Linxiao Chen, Iyad S. Ali, and Steven L Tait

This manuscript has been accepted after peer review and appears as an Accepted Article online prior to editing, proofing, and formal publication of the final Version of Record (VoR). This work is currently citable by using the Digital Object Identifier (DOI) given below. The VoR will be published online in Early View as soon as possible and may be different to this Accepted Article as a result of editing. Readers should obtain the VoR from the journal website shown below when it is published to ensure accuracy of information. The authors are responsible for the content of this Accepted Article.

**To be cited as:** *ChemCatChem* 10.1002/cctc.202000085

**Link to VoR:** <https://doi.org/10.1002/cctc.202000085>

*ChemCatChem*

**Bidentate N-based Ligands for Highly Reusable, Ligand-coordinated, Supported Pt  
Hydrosilylation Catalysts**

Dr. Linxiao Chen,<sup>†</sup> Mr. Iyad S. Ali, and Prof. Steven L. Tait\*

Dept. of Chemistry, Indiana University Bloomington, Bloomington, Indiana 47401, USA

\* E-mail: [tait@indiana.edu](mailto:tait@indiana.edu), Tel: +1-812-855-1302, Twitter: @StevenLTait

<sup>†</sup> Present address: Institute for Integrated Catalysis, Pacific Northwest National Laboratory,  
Richland, Washington 99352, USA

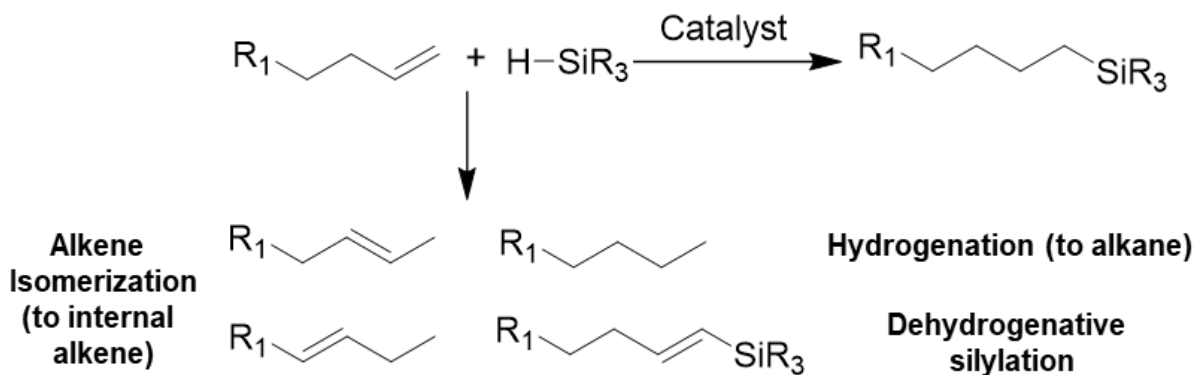
Accepted Manuscript

## Abstract

A significant challenge in designing supported metal-ligand catalysts for solution-phase reactions is the stabilization of the metal active sites against leaching into solution. Here, we examine alkene hydrosilylation reactions as model systems to improve the stability of highly dispersed Pt using a metal-ligand coordination strategy on high surface area oxide supports. By evaluating a series of bidentate N-based ligands, we demonstrate several design strategies to improve stability of the highly dispersed Pt<sup>2+</sup> centers against leaching, while maintaining a high level of catalytic activity, selectivity, and recyclability for alkene hydrosilylation batch reactions under mild conditions. These involve a bi-functional approach to ligand design, which considers interaction to the support and a well-defined coordination environment for the metal active site. Three strategies are reported: modifying ligands for stronger interaction with oxide surfaces, mixing ligands, and pre-depositing an “anchoring ligand” to the support before loading the metal-ligand catalyst. Each of these is successful in enhancing Pt recyclability. Particularly, two Pt-phenanthroline catalysts exhibit excellent reusability for multiple batch reaction cycles, due to high stability of the active Pt species. Addressing the active site leaching problem significantly enhances the utility of ligand-coordinated supported metal catalysts as highly stable and selective catalysts for solution-phase reactions.

## Introduction

Hydrosilylation, the addition of a Si–H bond to a multiple bond (particularly C=C, Scheme 1), has been of significant importance in silicon chemistry since its first report in 1947.<sup>[1]</sup> It serves as a versatile tool to produce various functionalized silicon-based polymers,<sup>[2]</sup> which have observed wide applications as lubricant oils<sup>[3]</sup> and as coating,<sup>[4]</sup> preceramic,<sup>[5]</sup> adhesive,<sup>[6]</sup> and sealing materials.<sup>[7]</sup> Hydrosilylation also offers solutions to silicone curing<sup>[4a, 8]</sup> and Si–C bond building in fine chemical synthesis.<sup>[9]</sup> Industrial hydrosilylation catalysts have long been dominated by homogeneous Pt complexes due to their superior activity over other metals.<sup>[10]</sup> Speier catalyst,  $\text{H}_2\text{PtCl}_6/\text{Pr-OH}$ ,<sup>[11]</sup> prevailed for decades before being replaced by the more active and selective Karstedt catalyst, a vinyl-siloxane  $\text{Pt}^0$  complex developed in 1970s.<sup>[12]</sup> One significant drawback of Karstedt catalyst is the formation of colloidal Pt, which deactivates the catalyst and reduces product quality.<sup>[4a, 13]</sup> The problem is further underscored by the high cost, volatile market, and uncertain future supply of Pt. Besides the Pt aggregation problem, side reactions of C=C isomerization and hydrogenation (Scheme 1) are difficult to avoid, and some important functional groups, such as epoxy,<sup>[14]</sup> are unstable under reaction conditions. Consequently, there is ongoing research effort to develop Pt hydrosilylation catalysts with improved selectivity and stability. Examples of recent progress include Pt-carbene complexes,<sup>[14-15]</sup> trinuclear alkyne  $\text{Pt}^0$  complexes,<sup>[16]</sup> and anti-sulfur-poisoning Pt catalysts.<sup>[17]</sup> Heterogeneous Pt catalysts, such as Pt nanoparticles,<sup>[13a-c]</sup>  $\text{PtO}_2$ ,<sup>[18]</sup> and supported Pt single-atoms,<sup>[19]</sup> have also inspired interest because they can be easily separated from the reaction mixture and recycled.



**Scheme 1.** General reaction scheme of hydrosilylation and common byproducts from alkene.

The quest has long existed for next-generation catalysts that combine the easy recovery of heterogeneous catalysts with the high metal utilization efficiency and selectivity of homogeneous catalysts. This has sparked growing interest in immobilized organometallic catalysts<sup>[20]</sup> and single-atom catalysts (SACs).<sup>[21]</sup> Both groups of catalysts fulfill the purpose of isolating single metal atoms on solid supports. The former offers higher metal loading and tunability, while the latter provides direct metal-support interaction, which is often crucial in catalysis. To combine desirable characters from both, we have developed a metal-ligand self-assembly strategy, first on single crystal surfaces in UHV<sup>[22]</sup> and then adapted to various high-surface-area oxide supports under ambient conditions<sup>[23]</sup> to create high-loading of ligand-stabilized and tunable noble metal sites with direct contact with the support. We demonstrated that Pt stabilized by 3,6-di-2-pyridyl-1,2,4,5-tetrazine (DPTZ, Figure 1a) on CeO<sub>2</sub> and MgO powders are atomically dispersed as Pt<sup>2+</sup>,<sup>[23a]</sup> and are much more active than supported Pt aggregates and existing Pt SACs for alkene hydrosilylation.<sup>[19a, 19b, 23b]</sup> Compared with the Karstedt catalyst, they improve selectivity, reduce Pt aggregation, and suppress the decomposition of epoxy groups.<sup>[23]</sup> Despite desired catalytic properties, Pt active sites on these catalysts partially leach into the solution during catalysis, limiting their recyclability and, hence, practical applications.

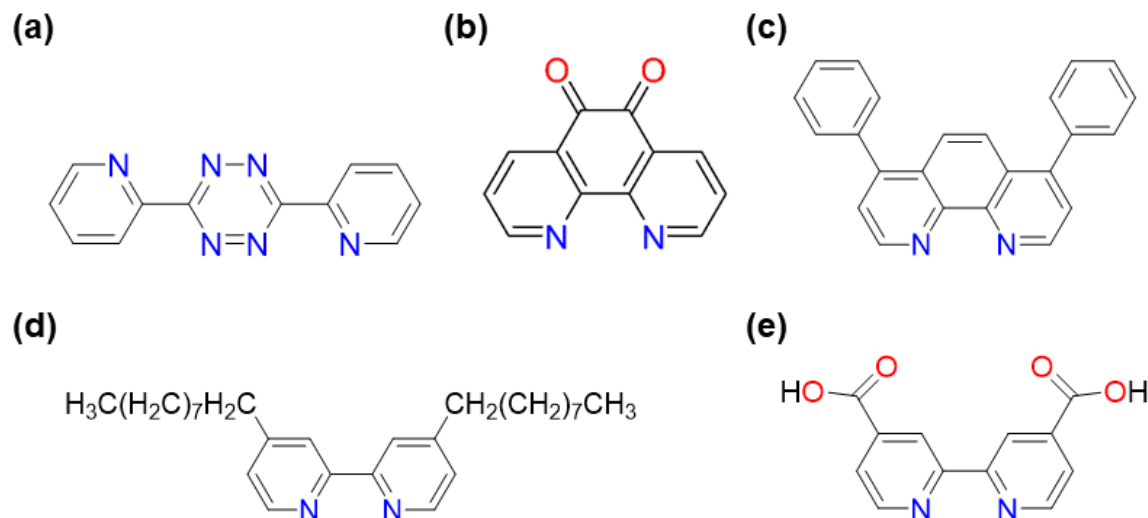


**Figure 1.** Structures of bidentate N-based ligands used in this work: (a) 3,6-(2-pyridyl)-1,2,4,5-tetrazine (DPTZ), (b) 1,10-phenanthroline-5,6-dione (PDO), (c) bathophenanthroline (BPhen), (d) 4,4'-dinonyl-2,2'-dipyridyl (C9BP), and (e) 2,2'-bipyridine-4,4'-dicarboxylic acid (4,4'-BPDCA).

Therefore, in this work, we introduce a series of bifunctional bidentate N-based ligands (Figure 1b-e), aiming to create supported Pt-ligand hydrosilylation catalysts with improved active site recyclability. Three approaches are discussed: replacing DPTZ with a different ligand, mixing DPTZ with another ligand, and pre-depositing an additional ligand as the “anchoring ligand.” The resulting Pt catalysts are evaluated with a model hydrosilylation reaction between 1-octene and dimethoxymethyl silane. We demonstrate that all three approaches are promising to mitigate the active site leaching problem, and present two catalysts with excellent reusability through multiple reaction cycles. Post-reaction characterization sheds light on the nature of active sites on these two catalysts. This work not only significantly improves the application potential of supported Pt-ligand hydrosilylation catalysts, it also expands the tool box for the synthesis of highly-dispersed noble metal catalysts on oxide supports.

## Experimental

**Synthesis of supported Pt-ligand catalysts.** The synthesis follows a metal-ligand self-assembly strategy reported in our previous publications.<sup>[23]</sup> For Pt-DPTZ/CeO<sub>2</sub>: 0.0108g (0.046 mmol) DPTZ (Sigma Aldrich, 96%) were completely dissolved in 25 mL 1-butanol (Alfa Aesar, 99%) by stirring for 20 min at room temperature. 0.3 g CeO<sub>2</sub> (BET surface area: 4.8 m<sup>2</sup>/g) were added to the pink DPTZ solution and the mixture was then stirred for 2 h at room temperature. 0.0080 g H<sub>2</sub>PtCl<sub>6</sub> · 6H<sub>2</sub>O (Alfa Aesar, 99.95% metal basis, 0.015 mmol, 1 wt % by Pt with respect to total catalyst mass; 3 eq. DPTZ with Pt) were dissolved in 5 mL 1-butanol. The Pt salt solution was then added to the CeO<sub>2</sub>/DPTZ/1-butanol mixture dropwise under stirring within 30 min. The mixture was covered and stirred for 24 h, then dried at room temperature under dry air flow overnight. The dried catalyst was washed with water, then dichloromethane (DCM) until powders did not show any pink color (all free DPTZ removed).

For Pt-PDO/CeO<sub>2</sub>, Pt-BPhen/CeO<sub>2</sub>, Pt-C9BP/CeO<sub>2</sub>, and Pt-4,4'-BPDCA/CeO<sub>2</sub>: the same procedure was followed, except that DPTZ was replaced by PDO (Sigma Aldrich, 98%), BPhen (Sigma Aldrich, 97%), C9BP (Alfa Aesar, 97%), or 4,4'-BPDCA (Alfa Aesar, 98%) and H<sub>2</sub>O was used instead of 1-butanol as the solvent in the case of PDO and 4,4'-BPDCA due to ligand solubility.

For Pt-BPhen+DPTZ/CeO<sub>2</sub> catalysts: DPTZ was replaced by a BPhen+DPTZ mixture of the same total mole quantity and various ratios.

For the catalysts with anchoring ligands, 0.07 mmol anchoring ligand was impregnated onto 0.5 g CeO<sub>2</sub> or MgO powder (BET surface area: ~5 m<sup>2</sup>/g) in a solvent (H<sub>2</sub>O for PDO and DCM for 4,4'-BPDCA),<sup>[24]</sup> then that ligand-modified support was used instead of pristine support in

the procedure described above. All supported Pt-ligand catalysts were yellow or light-yellow powders.

**General procedures for alkene hydrosilylation reactions.** For the 70 °C, 30 min reactions: 30 mg supported Pt catalysts were weighed and kept in an empty reaction tube with cap. 5 mmol dimethoxymethylsilane (Alfa Aesar, > 97%) and 6 mmol 1-octene (Alfa Aesar, > 97%) were weighed into another reaction tube, and 3 mL toluene (Macron, ACS grade) was added to the same tube. For the 60 °C, 20 min reactions, the amount of all chemicals was reduced to half. Both tubes were pre-heated in a water bath at the reaction temperature for 10 min before reactants and solvent were added into the tube with Pt catalysts. The tube was capped during the reaction to avoid evaporation of silane (low boiling point). After the reaction, the tube was cooled down quickly with cold water flow, the solid catalysts were centrifuged out for reuse or post-reaction characterization, and the liquid mixture was diluted to 25 mL for GC-MS measurements with an Agilent 6890N Gas Chromatograph and 5973 Inert Mass Selective Detector. Product yield was calculated from its response intensity at  $m/z = 203.2$  with respect to the response of internal standard decane (Sigma Aldrich, > 99%, ~ 0.15 g added to all standard and post-reaction solutions) at  $m/z = 142.2$  using calibration curves pre-made with standard solutions. The product used to make standard solutions was purchased from Sigma Aldrich ( $\geq 95.0\%$ ). The calibration curve exhibits an almost-perfect linear relationship between normalized GC-MS response and concentration over the concentration range relevant to the experiments reported here. For all samples we measured, the GC-MS response from decane is within 20% of standard solutions used in the calibration curves. Epoxy-containing alkene substrate hydrosilylation reactions occurred under 80 °C, 100 min conditions with 50 mg supported Pt catalyst weighed and kept in an empty reaction tube. 2.5 mmol trimethoxysilane

(Sigma Aldrich, 95%) and 3 mmol 4-vinyl-1-cyclohexene 1,2-epoxide isomers (Sigma Aldrich, 98%) were weighed into another reaction tube, and 1.5 mL toluene (Macron, ACS grade) was added to the same tube.

**Characterization of supported Pt-ligand catalysts.** X-ray photoemission spectroscopy (XPS) measurements were performed with a PHI Versaprobe II XP spectrometer using a monochromated Al X-ray source. A small amount of each powder sample was fixed onto a platen with double-sided tape. For CeO<sub>2</sub>-supported samples, XP spectra were collected for Pt 4f, N 1s, C 1s, Cl 2p, Ce 3d, and O 1s. For MgO-supported samples, the Ce 3d region was replaced by the Mg 2p region. An Ar<sup>+</sup> neutralizer was used to alleviate surface charging. The binding energy was corrected by calibration with the adventitious C 1s peak (284.8 eV). Inductively coupled plasma mass spectrometry (ICP-MS) measurements were performed with an Agilent 7700 quadrupole ICP-MS instrument. Solid catalysts were treated with aqua regia to dissolve all Pt before measurement. For solution samples, the solvent was evaporated first and then the residue was treated with aqua regia.

## Results and Discussion

### 1. Supported Pt-ligand catalysts with single bidentate N-based ligand

Previously we have reported oxide-supported Pt-DPTZ catalysts. Extensive characterization showed that Pt exist predominantly as isolated atoms stabilized by favorable Pt-DPTZ coordination, with direct contact with oxide supports. Therefore, these catalysts have been categorized as single-atom catalysts (SACs).<sup>[23]</sup> The SACs exhibit improvements over the commercial hydrosilylation catalyst (Karstedt catalyst) in selectivity, stability, and substrate

scope. Nevertheless, their application is challenged by low reusability due to active site leaching into solution during reaction. We have established that Pt-DPTZ coordination through the bidentate N binding pockets (Figure 1a) is highly stable, but the binding between Pt-DPTZ complexes and the oxide support is not.<sup>[23b]</sup> Consequently, we first replaced DPTZ with one of the following bifunctional bidentate N-based ligands: 1,10-phenanthroline-5,6-dione (PDO), bathophenanthroline (BPhen), 4,4'-dinonyl-2,2'-dipyridyl (C9BP), or 2,2'-bipyridine-4,4'-dicarboxylic acid (4,4'-BPDCA) (structures shown as Figure 1b-1e). Besides a bidentate N pocket, each ligand has additional functional groups for improved interaction with the oxide supports. Our hypothesis is that the replacement enhances the interaction between the Pt-ligand complex and the support to create active hydrosilylation catalysts with improved active site recyclability.

We synthesized supported Pt-ligand catalysts using the one-step metal-ligand impregnation method reported previously.<sup>[23a]</sup> In short,  $\text{H}_2\text{PtCl}_6 \cdot 6\text{H}_2\text{O}$  solution was added dropwise into pre-mixed ligand solution and  $\text{CeO}_2$ , followed by stirring, solvent evaporation, and rinsing (see experimental section for details). We chose  $\text{CeO}_2$  as the support because, in previous studies, we found higher catalytic activity and reusability with  $\text{CeO}_2$  than with other oxide supports.<sup>[23]</sup> Synthesis solvent was varied to ensure simultaneous dissolution of  $\text{H}_2\text{PtCl}_6 \cdot 6\text{H}_2\text{O}$  and the ligand (Table 1). 1 wt% Pt was added and the actual Pt loading, determined by inductively coupled plasma mass spectrometry (ICP-MS), was found to be in the range of 0.16 – 0.41 wt% (Table 1). On all fresh catalysts, the binding energy (BE) of the Pt  $4f_{7/2}$  XPS peak is consistent with  $\text{Pt}^{2+}$  (~72.8 eV, Table 1 and Figure 2). Figure 2 also shows that Pt  $4f$  XP spectra on most catalysts can be described well with a single  $\text{Pt}^{2+}$  component of similar FWHM (~2.1 eV), except for Pt-BPhen/ $\text{CeO}_2$ , on which the wide, asymmetric peak requires an additional  $\text{Pt}^{4+}$  component

for appropriate fitting (see SI for fitting details). Therefore, most Pt exist as highly dispersed  $\text{Pt}^{2+}$  cations and metallic Pt nanoparticles are not present. This is expected because the bidentate N pockets are suitable for Pt coordination and have sufficient oxidizing potential to stabilize dispersed single-atom  $\text{Pt}^{2+}$  on  $\text{CeO}_2$  and on  $\text{MgO}$ , as we have demonstrated previously.<sup>[23]</sup> On all catalysts, N (from ligands) and Cl (from  $\text{H}_2\text{PtCl}_6 \cdot 6\text{H}_2\text{O}$ ) are clearly identified by XPS (Figure S1, Table S2). N:Pt and Cl:Pt ratios are calculated from XPS peak areas and summarized in Table 1. The sum of the two ratios is at least 3, indicating Pt are highly coordinated with N and Cl. Besides, Pt need to coordinate with surface O to stay on  $\text{CeO}_2$ . The high coordination is consistent with the argument that Pt aggregates are not formed to a significant degree. In summary, XPS indicates that on these catalysts, Pt bind with ligands, Cl, and O from  $\text{CeO}_2$ , forming dispersed  $\text{Pt}^{2+}$  sites. We note that these XPS results are consistent with our previous studies of Pt-DPTZ SACs,<sup>[23a]</sup> for which EXAFS and STEM analysis conclusively proved a single-atom character of the metal sites, which implies that atomic dispersion is likely on the other catalysts reported here. However, due to a lack of comprehensive characterization, we refer to these as ligand-coordinated supported catalysts (LCSCs), rather than SACs.

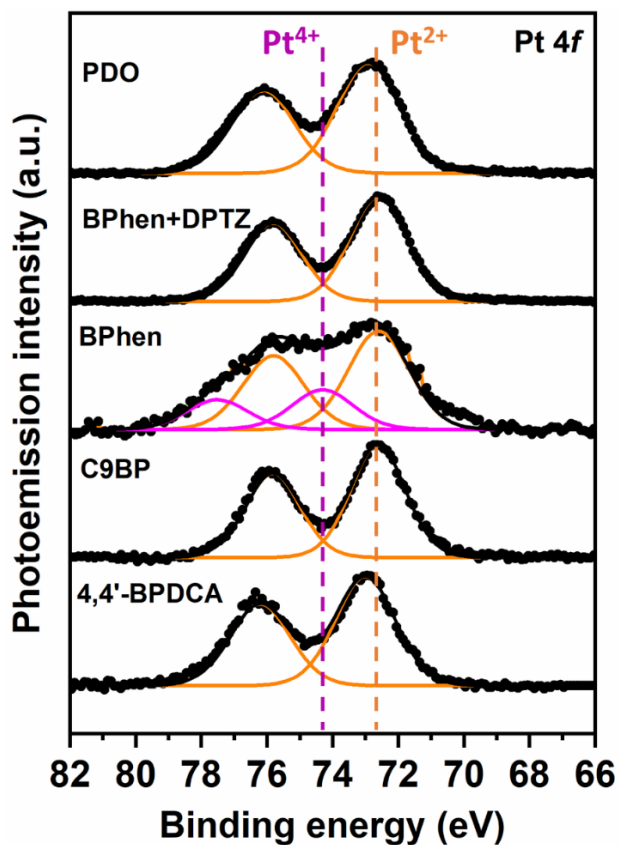


**Figure 2.** XP spectra of fresh (before reaction) CeO<sub>2</sub>-supported Pt-ligand LCSCs in the Pt 4f region. All spectra are normalized so that peaks have similar intensity for better peak shape comparison. All spectra except for Pt-BPhen/CeO<sub>2</sub> show a single Pt<sup>2+</sup> components (~72.8 eV). For Pt-BPhen/CeO<sub>2</sub>, a small fraction of Pt<sup>4+</sup> is also present.

**Table 1.** Synthesis and characterization of fresh CeO<sub>2</sub>-supported Pt-ligand catalysts for a series of ligands. Pt loading is calculated as wt % from ICP-MS. From XPS analysis, we measure Pt 4f<sub>7/2</sub> binding energy (BE) and molar ratios of N:Pt and Cl:Pt, calculated from peak area ratios and corrected for relative sensitivity factors.

Ligand	ICP Pt loading (wt %)	Pt 4f <sub>7/2</sub> BE (eV)	N:Pt	Cl:Pt	Synthesis solvent
DPTZ <sup>[a]</sup>	0.35	72.8	2.8	1.0	1-butanol
PDO	0.47	72.8	2.1	1.3	water
Bphen + DPTZ <sup>[b]</sup>	0.53	72.7	2.5	1.5	1-butanol
BPhen	0.29	72.8	1.4	2.8	1-butanol
C9BP	0.16	72.6	0.8	2.2	1-butanol
4,4'-BPDCA	0.41	72.9	4.6	1.1	water <sup>[c]</sup>

[a] Data on Pt-DPTZ/CeO<sub>2</sub> were previously published in reference 23b.

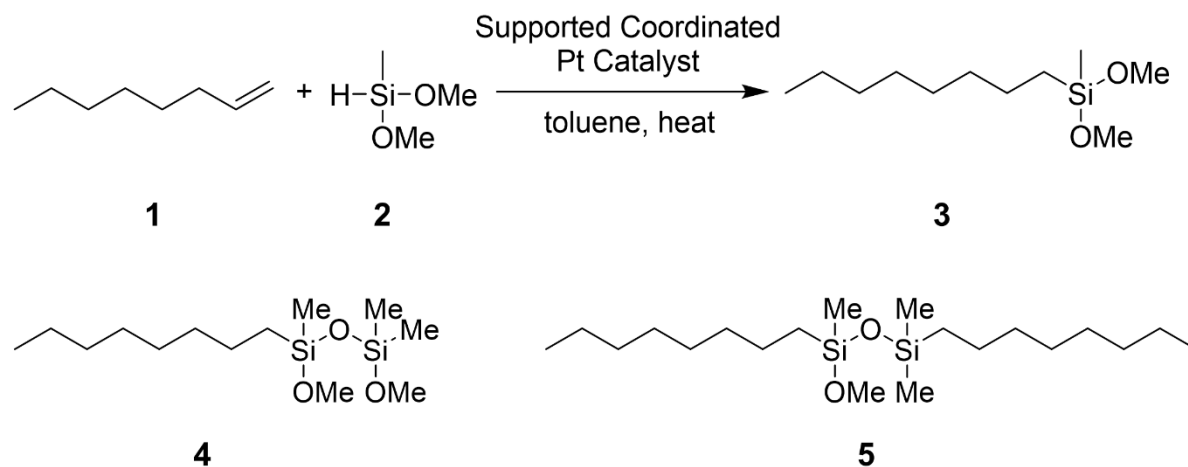
[b] The catalyst was synthesized using a mixture of BPhen and DPTZ (1:2 molar ratio).

[c] 4,4'-BPDCA was heated with water (to approximately 60 °C) to increase its solubility. The heat was turned off before adding Pt solution.

We tested these Pt LCSCs for a model hydrosilylation reaction between 1-octene (**1**) and dimethoxymethylsilane (**2**) (Scheme 2), under two conditions: 70 °C for 30 min and 60 °C for 20 min. The former is the “standard condition” to evaluate active site recyclability. The latter is for TON calculation and activity comparison, as it keeps the conversion of **2** far below 100%. Toluene was selected as the solvent for the reaction (Table S3). All catalysts, except Pt-4,4'-BPDCA/CeO<sub>2</sub>, exhibit catalytic activity under both conditions, yielding the anti-Markovnikov addition product **3**. Similar with most hydrosilylation catalysts, alkene isomerization and hydrogenation are unavoidable. Therefore, we performed all reactions with 1.2 eq. **1**. The most concentrated by-products are silane oligomers **4** and **5**, the concentration of which is very low

compared with **3** (see Figure S2 for a representative GC-MS spectrum). In addition, no Markovnikov addition product is observed, suggesting our catalysts are highly selective. The conversion of **2** is difficult to quantify precisely due to its volatility, so we instead used the yield of **3** to quantify catalytic activity.

Activity of all fresh catalysts at 70 °C, TON at 60 °C in the first 20 min, as well as total Pt recovery percentage (calculated from XPS Pt:Ce ratio, see SI for justification) after 1 reaction cycle are reported in Table 2. Both activity and Pt recyclability vary significantly with the choice of ligand, highlighting one unique advantage of the LCSCs: metal sites can be tuned by changing the ligand, as in organometallic complexes in homogeneous catalysis.



**Scheme 2.** Hydrosilylation reaction between 1-octene (**1**) and dimethoxymethylsilane (**2**) used to test Pt LCSCs, as well as structures of the two most important Si-containing by-products.

**Table 2.** Activity and total Pt recovery (by XPS) of Pt LCSCs.

Ligand	Yield <sup>[a]</sup> (%) 70 °C, 30 min	XPS Pt recovery <sup>[b]</sup> (%)		TON per Pt <sup>[c]</sup> (10 <sup>3</sup> ) 60 °C, 20 min
		1 cycle	3 cycles	
DPTZ	90 <sup>[d]</sup>	62	–	6.2
PDO	66	97	69	2.7
Bphen + DPTZ	83	86	23	2.2
Bphen	74	66	–	0.1
C9BP	23	27	–	10.2
4,4'-BPDCA	0	90	–	0

[a] Reaction condition:  $T = 70\text{ °C}$ ,  $t = 30\text{ min}$ , 30 mg catalyst, 6 mmol **1**, 5 mmol **2**, and 3 mL toluene.

[b] XPS Pt recovery was calculated based on Pt:Ce ratio compared with the fresh catalyst. Pt 4f XP spectra of post-reaction Pt-PDO/CeO<sub>2</sub> and Pt-BPhen+DPTZ/CeO<sub>2</sub> are included as a part of Figure 4, while others are presented as Figure S3.

[c] Reaction condition:  $T = 60\text{ °C}$ ,  $t = 20\text{ min}$ , 15 mg catalyst, 3 mmol **1**, 2.5 mmol **2**, and 1.5 mL toluene.

[d] Complete conversion of **2** was achieved in this reaction.

We examined the reusability of the catalyst with the highest Pt recovery percentage after 1 reaction cycle, Pt-PDO/CeO<sub>2</sub>, by recycling it for 4 cycles, and results are shown in Figure 3. For all reactions in Figure 3, the conversion of **2** is below 100%, and selectivity remains similar with the first cycle. Pt-PDO/CeO<sub>2</sub> shows excellent reusability, as its activity does not drop through the 4 cycles (~60% yield). In comparison, we have shown previously that product yield decreases quickly on Pt-DPTZ/CeO<sub>2</sub> once the conversion of **2** drops below 100% (Figure S4), due to active site leaching.<sup>[23b]</sup> Figure 3 strongly indicates that almost all active sites on Pt-PDO/CeO<sub>2</sub> can be recycled effectively, a drastic improvement over Pt-DPTZ/CeO<sub>2</sub>. Pt recovery percentage after the first cycle is also much higher on Pt-PDO/CeO<sub>2</sub> than Pt-DPTZ/CeO<sub>2</sub> (97% compared with 62%, Table 2). Minor Pt leaching does not deactivate Pt-PDO/CeO<sub>2</sub>, possibly because only relatively

inactive Pt sites are leached (see next paragraph). Besides Pt-PDO/CeO<sub>2</sub>, Pt-4,4'-BPDCA/CeO<sub>2</sub> exhibits enhanced Pt recyclability (90% after the first cycle) too, but it is not catalytically active. Pt-Bphen/CeO<sub>2</sub> and Pt-C9BP/CeO<sub>2</sub> exhibit underwhelming Pt recyclability (only 66% and 27%), possibly due to the low ligand loading (low N:Pt in Table 1) leading to relatively undercoordinated Pt. We recognize that Pt-PDO/CeO<sub>2</sub> is not as active as Pt-DPTZ/CeO<sub>2</sub> (lower yield and TON per Pt under identical reaction conditions), but the difference is within 3-fold. In practice, one can compensate for lower activity by using more catalysts, but active site leaching is more challenging, especially for expensive and environmental unfriendly noble metals. Therefore, from a practical perspective, significantly enhanced reusability is more valuable. For the hydrosilylation of epoxy-containing alkene shown in Scheme S1, Pt-PDO/CeO<sub>2</sub> exhibits similar selectivity (66%) with Pt-DPTZ/CeO<sub>2</sub> (71%) at 100% silane conversion (80 °C, 100 min),<sup>[23b]</sup> demonstrating desired stronger tolerance towards unstable groups than Karstedt catalyst (~ 50% selectivity).<sup>[14a, 23b]</sup>

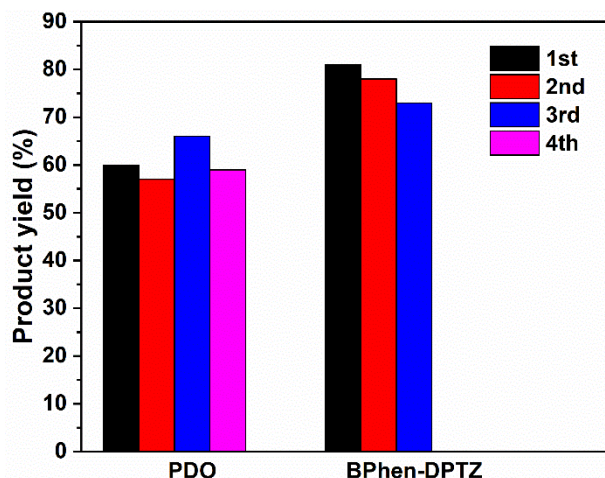


**Figure 3.** Reusability test results of Pt-PDO/CeO<sub>2</sub> (4 cycles) and Pt-BPhen+DPTZ/CeO<sub>2</sub> (3 cycles). Reaction condition:  $T = 70\text{ }^{\circ}\text{C}$ ,  $t = 30\text{ min}$ , 30 mg catalyst, 6 mmol **1**, 5 mmol **2**, and 3 mL toluene. After each reaction, the solid catalyst was centrifuged out and recycled. Both catalysts can be reused multiple times without significant loss of activity.

The highly reusable Pt-PDO/CeO<sub>2</sub> was characterized by XPS after the reaction to investigate its active sites. We found that most but not all Pt sites are recyclable, with 97% Pt recovered after 1 cycle and 69% recovered after 3 cycles (Table 2). ICP on post-reaction solution from the first cycle shows Pt equivalent with < 2% total Pt leaching, consistent with XPS. After the first cycle, Pt 4f XPS peak widens without significant shift in the BE, indicating broader oxidation state distribution centered around +2 (Figure 4a). Fitting (Figure 4a, Table 3) suggests two Pt components are formed: Pt<sup>(2-δ)+</sup> (~72.2 eV, red) and Pt<sup>(2+δ)+</sup> (~73.7 eV, green). This implies that at least two different Pt species exist on fresh Pt-PDO/CeO<sub>2</sub>. Although both appear to be Pt<sup>2+</sup> before catalysis, they evolve differently during catalysis, and hence the post-reaction oxidation state varies. Figure 4a and Table 3 also exhibit that after 3 cycles, the Pt<sup>(2+δ)+</sup> component does not change much, while the Pt<sup>(2-δ)+</sup> component drops, indicating the Pt leaching (~30% of total Pt) is mainly from the Pt<sup>(2-δ)+</sup> species. However, the partial loss of Pt<sup>(2-δ)+</sup> has negligible impacts on the activity (Figure 3). The lack of correlation between activity and the number of Pt<sup>(2-δ)+</sup> sites implies that Pt<sup>(2+δ)+</sup> sites are likely much more active than Pt<sup>(2-δ)+</sup>. We have hence demonstrated that although Pt leaching still occurs on Pt-PDO/CeO<sub>2</sub>, the main active sites are effectively recycled. We note that no Pt<sup>0</sup> are detected after catalysis, implying Pt remain highly dispersed. XPS also reveals that N:Pt ratio remains constant through 3 cycles (Table 3, Figure S5), and thus the Pt-PDO coordination is highly stable. In contrast, Cl:Pt ratio drops. The leaving of Cl has been previously reported on Pt-DPTZ SACs, which is associated with the catalyst activation.<sup>[23b]</sup> Cl might play a similar role on Pt-PDO/CeO<sub>2</sub>: it acts as a leaving group to open more coordination vacancies and activate Pt. In previous publications, we have established that with Pt-DPTZ ligand-stabilized SACs, the active Pt species may be generated during the reaction by temporary leaving the support, and then partially recovered by recombination with the support

after the reaction.<sup>[23b]</sup> This could also be a plausible mechanism for Pt-PDO/CeO<sub>2</sub>. Therefore, the good reusability does not necessarily prove that active Pt sites stay on CeO<sub>2</sub> throughout the reaction: it might result from the complete recovery of active Pt when the reaction is complete.

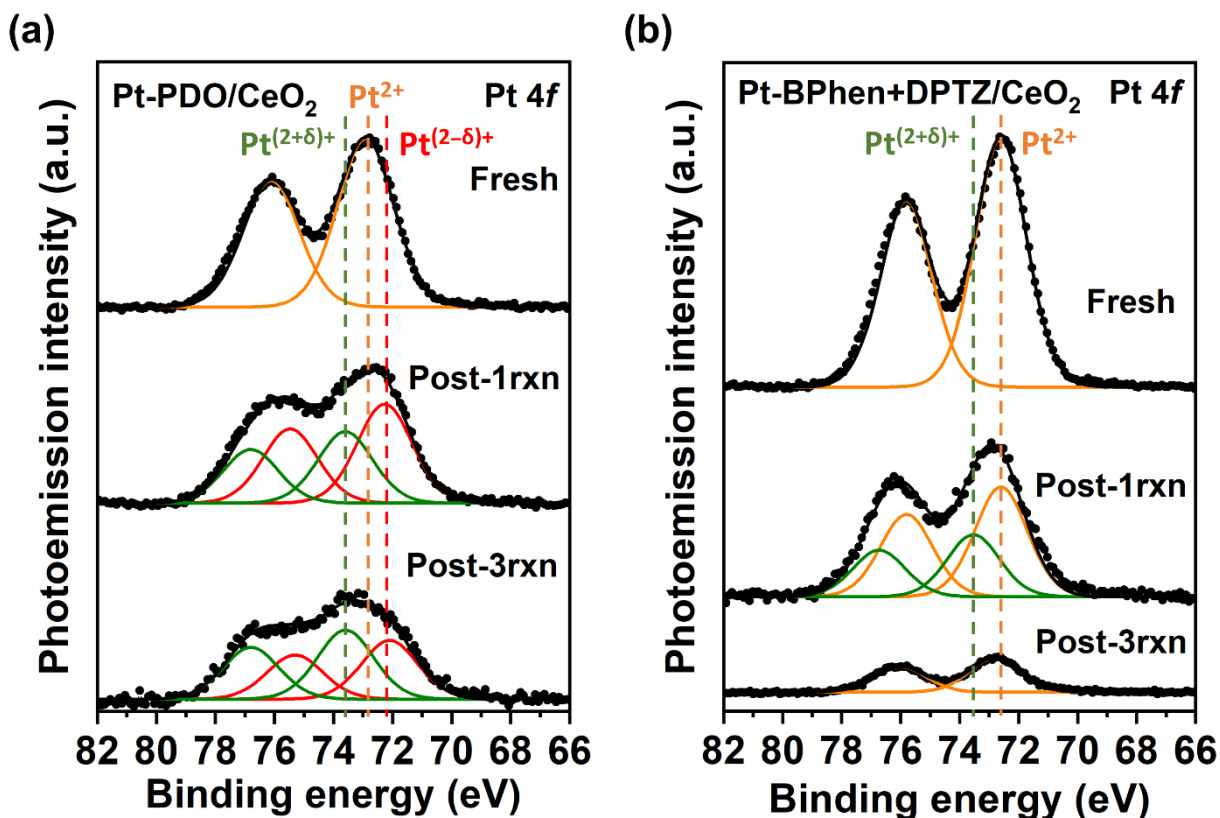


**Figure 4.** Fittings of Pt 4f XPS spectra of (a) Pt-PDO/CeO<sub>2</sub> and (b) Pt-BPhen+DPTZ/CeO<sub>2</sub>, including their fresh forms (top), after 1 reaction cycle (mid), and after 3 cycles (bottom). All spectra are normalized based on Ce 3d peak area so that the peak area reflects Pt concentration (Pt:Ce ratio) on the catalyst. See SI for discussion of fit components.

**Table 3.** Changes in relative Pt concentrations of various oxidation states, N:Pt ratio, and Cl:Pt ratio on Pt-PDO/CeO<sub>2</sub> and Pt-BPhen+DPTZ/CeO<sub>2</sub>.

Ligand	Catalyst status	Relative concentration <sup>[a]</sup>				N:Pt	Cl:Pt
		Pt <sup>(2-δ)+</sup>	Pt <sup>2+</sup>	Pt <sup>(2+δ)+</sup>	Total Pt		
PDO	Fresh	0	1	0	1	2.1	1.3
	post-1rxn	0.54	0	0.43	0.97	2	0.9
	post-3rxn	0.31	0	0.38	0.69	2.2	1
Bphen+DPTZ	Fresh	0	1	0	1	2.5	1.5
	post-1rxn	0	0.55	0.31	0.86	2.7	1.1
	post-3rxn	0	0.23	0	0.23	3	0.8

[a] Relative concentration of a Pt component on a sample was calculated based on the peak area from fittings (normalized to Ce 3d area of the same sample). For each catalyst, the total normalized Pt 4f peak area of its fresh form was defined as 1.

## 2. Enhancing recyclability of Pt-DPTZ/CeO<sub>2</sub> by combination with another ligand

We also attempted to improve active site recyclability of Pt-DPTZ SACs by mixing DPTZ with another ligand. The mixing ligand must be soluble in 1-butanol, the only solvent we discovered that dissolves DPTZ and H<sub>2</sub>PtCl<sub>6</sub> · 6H<sub>2</sub>O simultaneously. This excludes PDO and 4,4'-BPDCA. BPhen was chosen over C9BP for this study because when used alone, BPhen stabilizes Pt better than C9BP according to Table 2. This is potentially due to the benzene rings on BPhen offering stronger van der Waals interaction with CeO<sub>2</sub> than alkyl chains on C9BP. Besides, the phenanthroline ring on BPhen is more rigid than the bi-pyridyl ring on C9BP, possibly providing a more stable pocket for Pt binding. The synthesis procedure was adapted from the original Pt-DPTZ/CeO<sub>2</sub> recipe,<sup>[23a]</sup> with a fraction of DPTZ replaced by BPhen. We tested two BPhen:DPTZ molar ratios: 2:1 and 1:2. The former does not create active

hydrosilylation catalyst, so here we focus on the latter, referred to herein as Pt-BPhen+DPTZ/CeO<sub>2</sub>.

Pt-Bphen+DPTZ/CeO<sub>2</sub> exhibits significantly improved reusability over Pt-DPTZ/CeO<sub>2</sub>, as it only shows minimal activity drop in the first three cycles (from 81% yield to 73%, Figure 3). Pt recovery percentage after the first cycle is improved as well (86% compared with 62%, Table 2). The reusability of Pt-BPhen+DPTZ/CeO<sub>2</sub> is close to the most promising catalyst from the single-ligand strategy, Pt-PDO/CeO<sub>2</sub>. The two also exhibit similar activity at 60 °C (Table 2, TON = 2.2 and 2.7 × 10<sup>3</sup> respectively in the first 20 min), and selectivity with epoxy-containing alkene (63% and 66% at 100% silane conversion, respectively, for the reaction shown in Scheme S1). These results indicate that the mixed-ligand method offers another valid approach to alleviate the active site leaching problem. This strategy also provides an extra layer of tunability to the Pt sites, as catalyst properties can be modified by varying either ligand and the molar ratio between the two ligands.

Post-reaction XPS shows that, on Pt-BPhen+DPTZ, only a small fraction of Pt are the active sites. According to Table 3, Pt leaching is significant after three cycles (23% total Pt recovery). Nevertheless, the activity remains almost constant in Figure 3. This implies that, like the Pt-PDO/CeO<sub>2</sub> catalyst, leached Pt from Pt-BPhen+DPTZ/CeO<sub>2</sub> contribute little to the activity, and the main active sites are retained. Figure 2 and 4b show that fresh Pt-BPhen+DPTZ/CeO<sub>2</sub> also has predominately Pt<sup>2+</sup> species. After the first cycle, Pt 4f peak shifts to slightly higher BE and the peak widens. Fitting reveals that some Pt<sup>2+</sup> are converted into Pt<sup>(2+δ)+</sup> (Figure 4b, Table 3). After three cycles, both BE and FWHM of Pt 4f peak change back to values similar with the fresh catalyst, and the peak can again be described with a single Pt<sup>2+</sup> component. These results indicate that similar with Pt-PDO/CeO<sub>2</sub>, the Pt<sup>2+</sup> on fresh Pt-BPhen+DPTZ/CeO<sub>2</sub> also represents

multiple species of similar oxidation states. During 3 reaction cycles, some are converted into  $\text{Pt}^{(2+\delta)+}$  first and then leached away. Only a small fraction are highly stable, remaining on  $\text{CeO}_2$  with unchanged oxidation state. However, they are much more catalytically active than other species, and hence the catalyst shows good reusability overall. Table 3 and Figure S5 show that the decrease in Cl:Pt ratio after the reaction, which has been linked with Pt activation, is also observed on Pt-BPhen+DPTZ/ $\text{CeO}_2$ .<sup>[23b]</sup> N:Pt ratio does not decrease, again highlighting the strong binding between Pt and the bidentate N pockets. We also discovered that treating Pt-BPhen+DPTZ/ $\text{CeO}_2$  with only **2** in toluene (without **1**) at 70 °C leads to almost complete loss of Pt, N, Cl, (Figure S6) and the reaction activity. Therefore, despite the main active  $\text{Pt}^{2+}$  sites being highly recyclable under reaction conditions, interaction with silane without alkene induces significant leaching of active sites.

### 3. Using bidentate N-based ligands as anchoring ligands

The third strategy we explored is to use a bidentate N-based ligand to modify oxide supports for Pt-DPTZ LCSCs. The synthesis procedure includes two steps: an “anchoring” ligand was first deposited onto an oxide to form a ligand-modified oxide. Then, Pt-DPTZ LCSCs were synthesized using our usual procedure,<sup>[23a]</sup> with the anchoring-ligand-modified oxide as the support. We hypothesized that the ligand-modified supports can enhance catalyst reusability because the anchoring ligand can offer stronger interactions with Pt than surface O from pristine oxides. We tested the concept using PDO and 4,4'-BPDCa as anchoring ligands on both  $\text{CeO}_2$  and MgO (with similar surface area). The successful deposition of the anchoring ligand after the first step is verified by XPS N 1s peak area analysis (Figure S7), with higher loading on  $\text{CeO}_2$  than on MgO. Pt 4f XPS of both modified- $\text{CeO}_2$ -supported Pt-DPTZ catalysts show

predominantly  $\text{Pt}^{2+}$  (Figure 5), as on pristine  $\text{CeO}_2$ .<sup>[23a]</sup> On both MgO-supported catalysts, the Pt 4f peak is wider and more asymmetric (low-binding-energy tail), compared to the  $\text{CeO}_2$  catalysts, and fitting shows a small fraction of  $\text{Pt}^0$  (Figure 5), likely from small amount of Pt nanoparticles, which is not observed with Pt-DPTZ on pristine MgO.<sup>[23a]</sup>

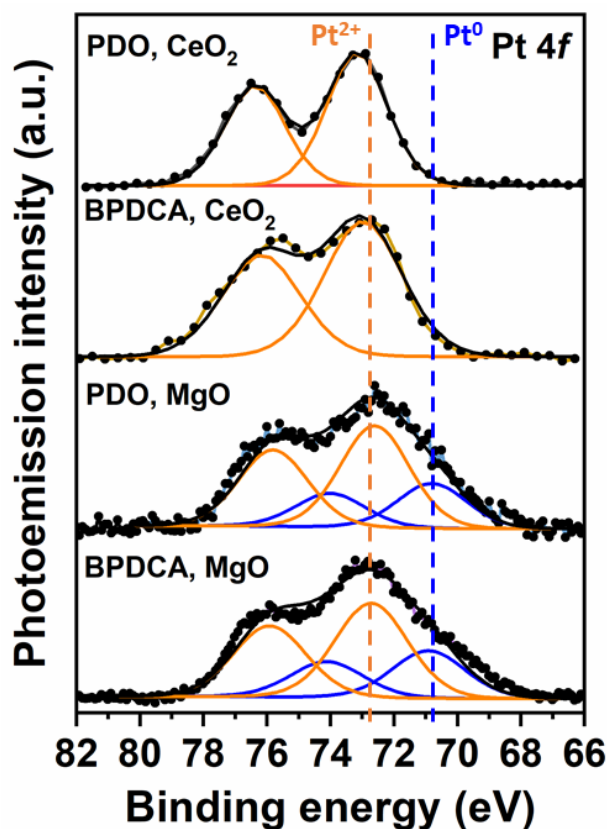


**Figure 5.** Fittings of Pt 4f XPS spectra of Pt-DPTZ LCSCs supported on an oxide ( $\text{CeO}_2$  or MgO) modified by an anchoring ligand (PDO or 4,4'-BPDCA). Each spectrum is labeled as “anchoring ligand, support”, and BPDCA refers to 4,4'-BPDCA. All spectra are normalized so that peaks are of similar intensity for better peak shape comparison. Pt exist predominantly as  $\text{Pt}^{2+}$  on modified  $\text{CeO}_2$ , while a small fraction of  $\text{Pt}^0$  is observed on modified MgO.

The activity and Pt recyclability of these catalysts are reported in Table 4. The enhancement in Pt recyclability by the anchoring ligand is clearly observed on both supports, as Pt recovery increases on ligand-modified supports compared with pristine supports. Meanwhile, activity

drops, the extent of which varies. Despite the activity loss, Table 4 shows that when the proper anchoring ligand and support are used (PDO and CeO<sub>2</sub>), this strategy can create Pt-DPTZ LCSCs with significantly improved Pt recyclability (from 62% to 82%) while maintaining acceptable activity (68% yield at 70 °C for 30 min, similar with Pt-PDO/CeO<sub>2</sub> in Table 2). Therefore, the anchoring ligand method is a promising approach. Pt recyclability is better on CeO<sub>2</sub> than on MgO, likely due to the higher anchoring ligand coverage on CeO<sub>2</sub> (Figure S7).

**Table 4.** Activity and total Pt recovery (after 1 reaction cycle) of Pt-DPTZ LCSCs supported on anchoring-ligand-modified oxides.

Support	Anchoring ligand	Yield (%)	XPS Pt recovery (%)
CeO <sub>2</sub> <sup>[a]</sup>	No anchoring ligand	90 <sup>[c, d]</sup>	62
	PDO	68	82
	4,4'-BPDCA	0	91
MgO <sup>[b]</sup>	No anchoring ligand	95 <sup>[c, d]</sup>	32
	PDO	49	36
	4,4'-BPDCA	93 <sup>[c]</sup>	47

[a] Reaction condition:  $T = 70\text{ }^{\circ}\text{C}$ ,  $t = 30\text{ min}$ , 30 mg catalyst, 6 mmol **1**, 5 mmol **2**, and 3 mL toluene.

[b] Reaction condition:  $T = 75\text{ }^{\circ}\text{C}$ ,  $t = 120\text{ min}$ , 30 mg catalyst, 6 mmol **1**, 5 mmol **2**, and 3 mL toluene.

[c] Complete conversion of **2** was achieved in these reactions.

[d] Data on unmodified Pt-DPTZ SACs were previously published in reference 23b.

We note that, in some cases, the activity loss with the anchoring ligand is too significant. For example, 4,4'-BPDCA leads to complete deactivation on CeO<sub>2</sub>. 5,5'-BPDCA, another ligand with the same -COOH groups but at different positions (Figure S8a), does the same. Control experiments show that modifying CeO<sub>2</sub> with trifluoroacetic acid (Figure S8b), a ligand with a -COOH group but without the bidentate N pocket to anchor Pt-DPTZ, does not completely

deactivate the catalyst. Consequently, the deactivation cannot be simply attributed to  $-\text{COOH}$  groups occupying certain catalytically relevant sites on  $\text{CeO}_2$ , such as oxygen defects. We suspect that the deactivation might be related to strong interactions between  $-\text{COOH}$  groups and  $\text{CeO}_2$  forcing BPDCA to stand up, pushing Pt away from the support. The loss of Pt-support interaction may impact the electronic structure of Pt enough to deactivate the site. We have demonstrated previously that surface O temporarily detach from Pt during catalysis, acting as “reversible leaving groups,”<sup>[23b]</sup> so the lack of Pt-support binding may also reduce the number of leaving groups, so that the Pt is over-coordinated. The sensitivity of the metal center to the local coordination environment is a topic of ongoing study and interest.

## Conclusions

In this work, we reported a series of ligand-coordinated supported Pt hydrosilylation catalysts with various bidentate N-based ligands, designed to improve catalyst recyclability over previous Pt-DPTZ SACs. These heterogeneous catalysts mostly contain highly dispersed  $\text{Pt}^{2+}$  sites, and are active for alkene hydrosilylation under mild conditions with high selectivity. We demonstrated three approaches to alleviate the active site leaching problem on the original Pt-DPTZ SACs. First, by replacing DPTZ with a ligand containing additional functional groups that offer strong interactions with oxide supports, we developed Pt-PDO/ $\text{CeO}_2$ , a catalyst with steady activity through four reaction cycles and much less Pt leaching. A  $\text{Pt}^{(2+\delta)+}$  species converted from  $\text{Pt}^{2+}$  is likely the active site. Second, we discovered that mixing DPTZ with BPhen, a ligand providing additional van der Waals interaction with the support, leads to a highly reusable catalyst Pt-BPhen+DPTZ/ $\text{CeO}_2$ , which shows only 10% activity loss after three reaction cycles, due to a  $\text{Pt}^{2+}$  species that is highly active and stable, despite accounting for only a small fraction

of total Pt. Finally, we showed that modifying oxide supports with an anchoring ligand enhances Pt recyclability on Pt-DPTZ SACs. All three strategies are promising to enhance the reusability of supported Pt-ligand single-atom hydrosilylation catalysts, while maintaining high activity and selectivity. Meanwhile, new development in synthesis methods reported here also expands future opportunities to fine-tune metal centers in these catalysts towards desired properties.

### **Acknowledgement**

This work was supported by the U. S. Department of Energy, Office of Basic Energy Sciences, Chemical Sciences program, DE-SC0016367. XPS measurements were carried out at Indiana University (IU) Nanoscale Characterization Facility with assistance from Dr. Yaroslav Lasovyj, Dr. Xuemei Zhou, and Eman Wasim. GC-MS measurements were carried out at the IU Mass Spectrometry Facility with assistance from Dr. Jonathan A. Karty. ICP-MS measurements were performed at IU Department of Earth & Atmospheric Sciences with assistance from Dr. Laura Wasylenki and Benjamin S. Underwood.

### **Conflicts of interest**

There are no conflicts of interest to declare.

**Keywords:** Heterogeneous Catalysis, Hydrosilylation, Platinum, N Ligands, X-ray Photoemission Spectroscopy

## References

- [1] L. Sommer, E. Pietrusza, F. Whitmore, *J. Am. Chem. Soc.* **1947**, *69*, 188-188.
- [2] a) O. R. Pierce, Y. K. Kim, *Rubber Chem. Technol.* **1971**, *44*, 1350-1362; b) B. Marciniak, E. Walczuk, P. Blazejewska-Chadyniak, D. Chadyniak, M. Kujawa-Welten, S. Krompiec, N. Auner, J. Weiss, *Wiley VCH, Weinheim* **2003**; c) Y. Morita, S. Tajima, H. Suzuki, H. Sugino, *J. Appl. Polym. Sci.* **2006**, *100*, 2010-2019; d) E. Beyou, P. Babin, B. Bennetau, J. Dunogues, D. Teyssie, S. Boileau, *J. Polym. Sci., Part A: Polym. Chem.* **1994**, *32*, 1673-1681; e) C. Iojoiu, M. J. Abadie, V. Harabagiu, M. Pinteala, B. C. Simionescu, *Eur. Polym. J.* **2000**, *36*, 2115-2123; f) Z. Li, J. Qin, Z. Yang, C. Ye, *J. Appl. Polym. Sci.* **2004**, *94*, 769-774; g) A. Sellinger, R. M. Laine, V. Chu, C. Viney, *J. Polym. Sci., Part A: Polym. Chem.* **1994**, *32*, 3069-3089; h) D. B. Drazkowski, A. Lee, T. S. Haddad, D. J. Cookson, *Macromolecules* **2006**, *39*, 1854-1863; i) A. Tuchbreiter, H. Werner, L. H. Gade, *Dalton Trans.* **2005**, 1394-1402.
- [3] H. Maciejewski, A. Wawrzyńczak, M. Dutkiewicz, R. Fiedorow, *J. Mol. Catal. A: Chem.* **2006**, *257*, 141-148.
- [4] a) D. Troegel, J. Stohrer, *Coord. Chem. Rev.* **2011**, *255*, 1440-1459; b) B. Marciniak, *Hydrosilylation: a comprehensive review on recent advances, Vol. 1*, Springer Science & Business Media, **2008**; c) T. Ganicz, T. Pakuła, W. A. Stańczyk, *J. Organomet. Chem.* **2006**, *691*, 5052-5055.
- [5] a) B. Boury, R. J. Corriu, D. Leclercq, P. H. Mutin, J. M. Planeix, A. Vioux, *Organometallics* **1991**, *10*, 1457-1461; b) A. Mori, H. Sato, K. Mizuno, T. Hiyama, K. Shintani, Y. Kawakami, *Chem. Lett.* **1996**, *25*, 517-518.

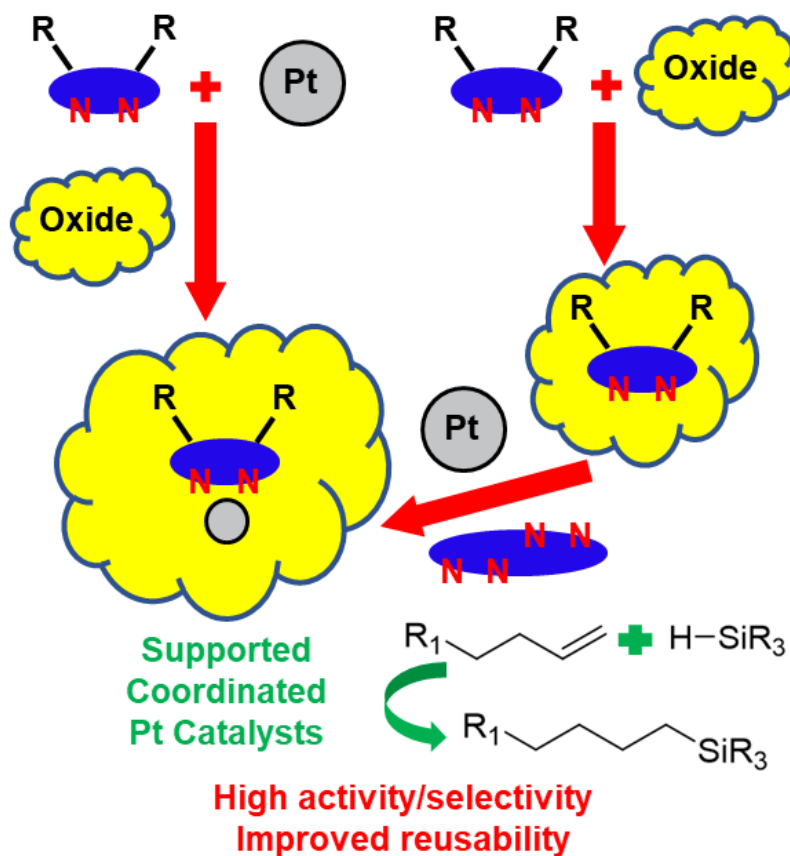
- [6] a) M. J. O'brien, US Patent 6,531,540, **2003**; b) C. Herzig, B. Deubzer, D. Huettner, US Patent 5,241,034, **1993**.
- [7] a) H. Jyono, H. Odaka, H. Ito, H. Iwakiri, US Patent 6,444,775, **2002**; b) T. Watabe, T. Matsumoto, T. Onoguchi, K. Tsuruoka, US Patent 6,207,766, **2001**.
- [8] P. Jerschow, *Silicone elastomers, Vol. 137*, Smart Publications, **2001**.
- [9] a) R. H. Morris, *Chem. Soc. Rev.* **2009**, 38, 2282-2291; b) B. K. Langlotz, H. Wadepohl, L. H. Gade, *Angew. Chem. Int. Ed.* **2008**, 47, 4670-4674; c) S. C. Bart, E. Lobkovsky, P. J. Chirik, *J. Am. Chem. Soc.* **2004**, 126, 13794-13807; d) I. Vankelecom, P. Jacobs, *Catal. Today* **2000**, 56, 147-157.
- [10] a) M. Xue, J. Li, J. Peng, Y. Bai, G. Zhang, W. Xiao, G. Lai, *Appl. Organomet. Chem.* **2014**, 28, 120-126; b) M. Igarashi, T. Matsumoto, T. Kobayashi, K. Sato, W. Ando, S. Shimada, M. Hara, H. Uchida, *J. Organomet. Chem.* **2014**, 752, 141-146; c) H. Dong, Y. Jiang, H. Berke, *J. Organomet. Chem.* **2014**, 750, 17-22; d) J. Y. Wu, B. N. Stanzl, T. Ritter, *J. Am. Chem. Soc.* **2010**, 132, 13214-13216; e) P. B. Glaser, T. D. Tilley, *J. Am. Chem. Soc.* **2003**, 125, 13640-13641; f) S. Nozakura, S. Konotsune, *Bull. Chem. Soc. Jpn.* **1956**, 29, 326-331; g) L. Bareille, S. Becht, J. L. Cui, P. Le Gendre, C. Moïse, *Organometallics* **2005**, 24, 5802-5806; h) S. Harder, J. Brettar, *Angew. Chem. Int. Ed.* **2006**, 45, 3474-3478; i) V. Leich, T. P. Spaniol, L. Maron, J. Okuda, *Chem. Commun.* **2014**, 50, 2311-2314.
- [11] J. L. Speier, J. A. Webster, G. H. Barnes, *J. Am. Chem. Soc.* **1957**, 79, 974-979.
- [12] B. Karstedt, US Patent 3,775,452, **1973**.
- [13] a) T. Galeandro-Diamant, M.-L. Zanota, R. Sayah, L. Veyre, C. Nikitine, C. de Bellefon, S. Marrot, V. Meille, C. Thieuleux, *Chem. Commun.* **2015**, 51, 16194-16196; b) B. P.

- Chauhan, J. S. Rathore, *J. Am. Chem. Soc.* **2005**, *127*, 5790-5791; c) Y. Bai, S. Zhang, Y. Deng, J. Peng, J. Li, Y. Hu, X. Li, G. Lai, *J. Colloid Interface Sci.* **2013**, *394*, 428-433; d) J. Stein, L. Lewis, Y. Gao, R. Scott, *J. Am. Chem. Soc.* **1999**, *121*, 3693-3703; e) T. K. Meister, K. Riener, P. Gigler, J. r. Stohrer, W. A. Herrmann, F. E. Kühn, *ACS Catal.* **2016**, *6*, 1274-1284.
- [14] a) I. E. Markó, S. Stérin, O. Buisine, G. Mignani, P. Branlard, B. Tinant, J.-P. Declercq, *Science* **2002**, *298*, 204-206; b) I. E. Markó, S. Sterin, O. Buisine, G. Berthon, G. Michaud, B. Tinant, J. P. Declercq, *Adv. Synth. Catal.* **2004**, *346*, 1429-1434.
- [15] a) J. C. Bernhammer, H. V. Huynh, *Organometallics* **2013**, *33*, 172-180; b) J. J. Dunsford, K. J. Cavell, B. Kariuki, *J. Organomet. Chem.* **2011**, *696*, 188-194; c) M. A. Taige, S. Ahrens, T. Strassner, *J. Organomet. Chem.* **2011**, *696*, 2918-2927.
- [16] B. Marciniak, K. Posala, I. Kownacki, M. Kubicki, R. Taylor, *ChemCatChem* **2012**, *4*, 1935-1937.
- [17] C. M. Downing, H. H. Kung, *Catal. Commun.* **2011**, *12*, 1166-1169.
- [18] N. Sabourault, G. Mignani, A. Wagner, C. Mioskowski, *Org. Lett.* **2002**, *4*, 2117-2119.
- [19] a) Y. J. Chen, S. F. Ji, W. M. Sun, W. X. Chen, J. C. Dong, J. F. Wen, J. Zhang, Z. Li, L. R. Zheng, C. Chen, Q. Peng, D. S. Wang, Y. D. Li, *J. Am. Chem. Soc.* **2018**, *140*, 7407-7410; b) Y. Zhu, T. Cao, C. Cao, J. Luo, W. Chen, L. Zheng, J. Dong, J. Zhang, Y. Han, Z. Li, C. Chen, Q. Peng, D. Wang, Y. Li, *ACS Catal.* **2018**, *8*, 10004-10011; c) X. Cui, K. Junge, X. Dai, C. Kreyenschulte, M.-M. Pohl, S. Wohlrab, F. Shi, A. Brückner, M. Beller, *ACS Central Science* **2017**, *3*, 580-585.
- [20] a) K. M. Mantovani, J. F. Stival, F. Wypych, L. Bach, P. G. P. Zamora, M. L. Rocco, S. Nakagaki, *J. Catal.* **2017**, *352*, 442-451; b) M. Rimoldi, D. Fodor, J. A. van Bokhoven,

- A. Mezzetti, *Chem. Comm.* **2013**, *49*, 11314-11316; c) W. Xu, Y. Li, B. Yu, J. Yang, Y. Zhang, X. Chen, G. Zhang, Z. Gao, *J. Solid State Chem.* **2015**, *221*, 208-215; d) L. Chen, S. Rangan, J. Li, H. Jiang, Y. Li, *Green Chemistry* **2014**, *16*, 3978-3985.
- [21] a) Z. Huang, X. Gu, Q. Cao, P. Hu, J. Hao, J. Li, X. Tang, *Angew. Chem.* **2012**, *124*, 4274-4279; b) E. Fako, Z. Lodziana, N. Lopez, *Catal. Sci. Technol.* **2017**, *7*, 4285-4293; c) Y. X. Chen, Z. W. Huang, Z. Ma, J. M. Chen, X. F. Tang, *Catal. Sci. Technol.* **2017**, *7*, 4250-4258; d) G. Vilé, D. Albani, M. Nachtegaal, Z. Chen, D. Dontsova, M. Antonietti, N. López, J. Pérez-Ramírez, *Angew. Chem. Int. Ed.* **2015**, *54*, 11265-11269; e) W. Xu, B. Yu, Y. Zhang, X. Chen, G. Zhang, Z. Gao, *Appl. Surf. Sci.* **2015**, *325*, 227-234; f) P. Ji, K. Manna, Z. Lin, A. Urban, F. X. Greene, G. Lan, W. Lin, *J. Am. Chem. Soc.* **2016**, *138*, 12234-12242; g) N. M. Schweitzer, B. Hu, U. Das, H. Kim, J. Greeley, L. A. Curtiss, P. C. Stair, J. T. Miller, A. S. Hock, *ACS Catal.* **2014**, *4*, 1091-1098; h) H. Sohn, J. Camacho-Bunquin, R. Langeslay, P. Ignacio-de Leon, J. Niklas, O. Poluektov, C. Liu, J. Connell, D. Yang, J. Kropf, *Chem. Commun.* **2017**; i) B. Qiao, A. Wang, X. Yang, L. F. Allard, Z. Jiang, Y. Cui, J. Liu, J. Li, T. Zhang, *Nature chemistry* **2011**, *3*, 634-641; j) Z. Li, S. Ji, Y. Liu, X. Cao, S. Tian, Y. Chen, Z. Niu, Y. Li, *Chem. Rev.* **2019**; k) L. DeRita, S. Dai, K. Lopez-Zepeda, N. Pham, G. W. Graham, X. Pan, P. Christopher, *J. Am. Chem. Soc.* **2017**, *139*, 14150-14165; l) J. Liu, *ACS Catal.* **2017**, *7*, 34-59; m) X. Cui, W. Li, P. Ryabchuk, K. Junge, M. Beller, *Nat. Catal.* **2018**, *1*, 385-397; n) L. Liu, D. M. Meira, R. Arenal, P. Concepcion, A. V. Puga, A. Corma, *ACS Catal.* **2019**, 10626-10639.
- [22] a) D. Skomski, C. D. Tempas, B. J. Cook, A. V. Polezhaev, K. A. Smith, K. G. Caulton, S. L. Tait, *J. Am. Chem. Soc.* **2015**, *137*, 7898-7902; b) D. Skomski, C. D. Tempas, G. S. Bukowski, K. A. Smith, S. L. Tait, *J. Chem. Phys.* **2015**, *142*, 101913; c) D. Skomski, C.

- D. Tempas, K. A. Smith, S. L. Tait, *J. Am. Chem. Soc.* **2014**, *136*, 9862-9865; d) C. D. Tempas, D. Skomski, B. J. Cook, D. Le, K. A. Smith, T. S. Rahman, K. G. Caulton, S. L. Tait, *Chem. Eur. J.* **2018**, *24*, 15852-15858; e) C. G. Williams, M. Wang, D. Skomski, C. D. Tempas, L. L. Kesmodel, S. L. Tait, *J. Phys. Chem. C* **2017**; f) T. W. Morris, I. J. Huerfano, M. Wang, D. L. Wisman, A. C. Cabelof, N. U. Din, C. D. Tempas, D. Le, A. V. Polezhaev, T. S. Rahman, K. G. Caulton, S. L. Tait, *Chem. Eur. J.* **2019**, *25*, 5565-5573.
- [23] a) L. Chen, G. E. Sterbinsky, S. L. Tait, *J. Catal.* **2018**, *365*, 303-312; b) L. Chen, I. S. Ali, G. E. Sterbinsky, J. T. L. Gamler, S. E. Skrabalak, S. L. Tait, *ChemCatChem* **2019**, *11*, 2843-2854.
- [24] L. Chen, V. Agrawal, S. L. Tait, *Catalysis Science & Technology* **2019**, *9*, 1802-1815.

## Table of Contents entry



Bi-functional ligands with bidentate N pockets are investigated to create oxide-supported ligand-coordinated Pt catalysts for alkene hydrosilylation. Three synthesis approaches are explored based on previously reported Pt-DPTZ SACs. These catalysts show significantly enhanced reusability over existing similar catalysts while maintaining high activity and selectivity.